Catalysis Letters (2023) 153:1756–1772
https://doi.org/10.1007/s10562-022-04096-y

Soybean Oil Epoxidation Catalyzed by a Functionalized Metal–Organic Framework with Active Dioxo-Molybdenum (VI) Centers

Diana C. Martínez R.[1,3] · Carlos A. Trujillo[2] · Jose G. Carriazo[3] · Nelson J. Castellanos[1,3]

Received: 3 April 2022 / Accepted: 26 June 2022 / Published online: 23 July 2022

Abstract

In this work, a functionalized gallium metal–organic framework with active dioxo-molybdenum (VI) centers was evaluated as a catalyst in the epoxidation of soybean oil using tert-butyl-hydroperoxide as an oxidizing agent. The influence of the reaction time, temperature, and concentration of the oxidizing agent was studied, and it was demonstrated that the highest epoxide selectivity was obtained at 110 °C after 4 h of reaction (29% conversion and 91% selectivity) using a soybean oil/oxidizing agent ratio of 1/2. The stability of the metal–organic framework was confirmed by infrared spectroscopy, X-ray powder diffraction, thermogravimetric analysis, scanning electron microscopy, and energy-dispersive X-ray spectroscopy EDS. The stability tests demonstrated that the catalyst could be reused in the catalytic process for the recovery of vegetable oils.

✉ Nelson J. Castellanos
njcastellanosm@unal.edu.co

[1] Departamento de Química, Facultad de Ciencias, Estado Sólido y Catálisis Ambiental (ESCA), Universidad Nacional de Colombia, Carrera 30 No. 45-03, Bogotá 111321, Colombia

[2] Departamento de Química, Facultad de Ciencias, Laboratorio de Catálisis Heterogénea (LCH), Universidad Nacional de Colombia, Carrera 30 No. 45-03, Bogotá 111321, Colombia

[3] Departamento de Química, Facultad de Ciencias, Laboratorio de Diseño y Reactividad de Estructuras Sólidas (Lab-DRES, 125), Universidad Nacional de Colombia, Carrera 30 No. 45-03, Bogotá 111321, Colombia

Graphical Abstract

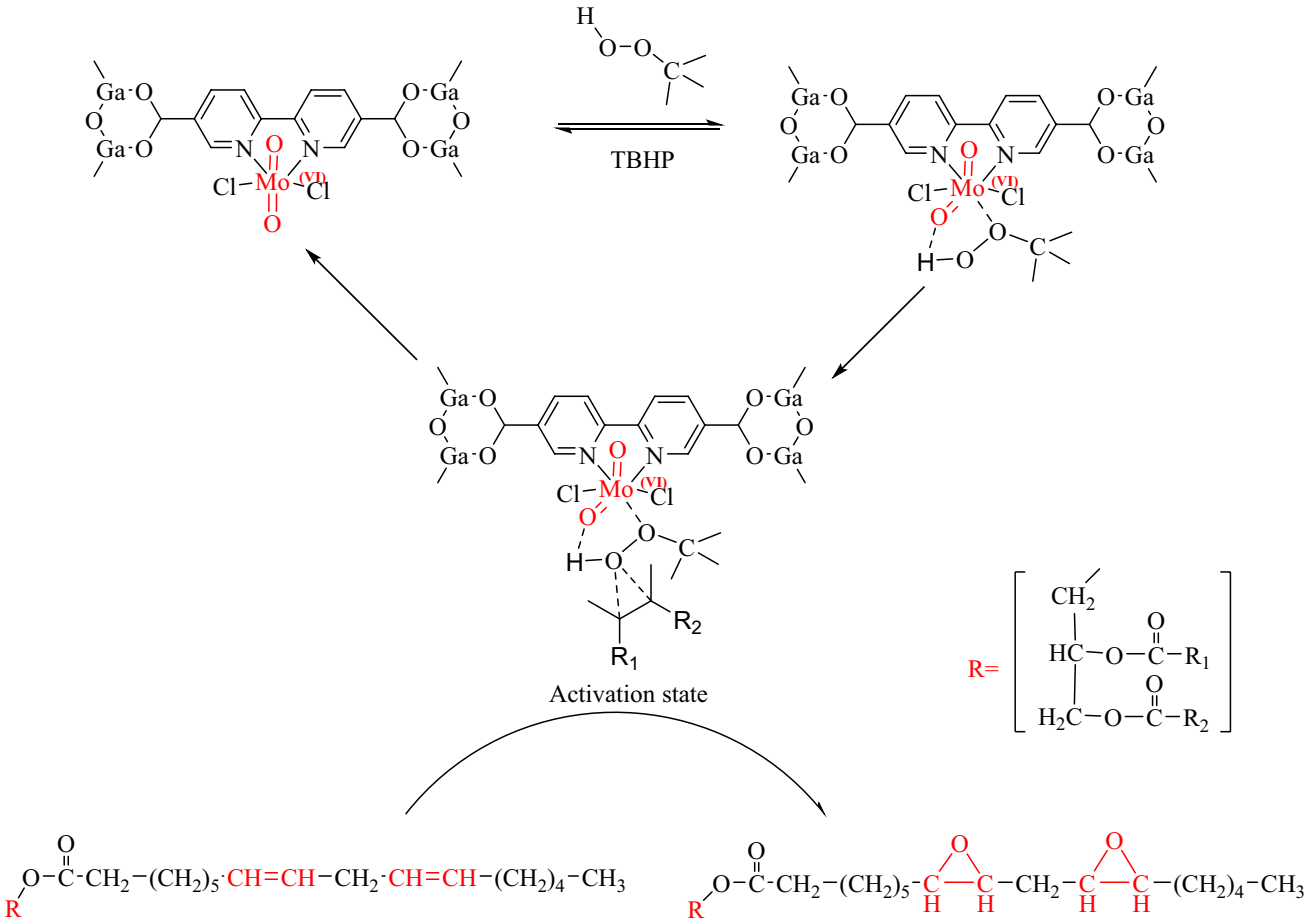

Keywords Vegetable oils epoxidation · Metal–organic frameworks · Dioxo-molybdenum(VI) complexes

1 Introduction

Renewable raw materials for the production of biodegradable materials have become a fundamental strategy for a global sustainable future alternative to replace the use of oil and its derivatives, which represent one of the main sources of environmental pollution [1–3]. Vegetable oils are one of the most promising, cheap, and available types of renewable sources, currently becoming the focus of interest for the chemical industry, and considered as environmentally friendly starting materials for the development of new processes and products [4–6].

Vegetable oils are products extracted from the seeds and/or fruits of oleaginous plants such as soybeans, palm and sunflower [2, 3], which at the molecular level are made up of triglycerides, glycerol esters, and straight-chain fatty acids [7]. They are currently of great importance for industry due to their use in food and in the production of biofuels [4, 8–10]. Because of the presence of unsaturation in their chemical structure, much research is focused on obtaining EVOs, which are used nowadays as precursors for the synthesis of polyurethane foams [11–14], plasticizers-stabilizers of high-use polymers such as PVC [15–18] and as essential components for obtaining biodegradable lubricants [19, 20].

In industry, EVOs are obtained through the Prileschajew reaction, which is a homogeneous classical epoxidation reaction catalyzed by percarboxylic acids (R–COO–OH) synthesized in situ from mineral acids, and used as oxidizing agents [21]. As highly toxic reagents are used in this reaction, the generated chemical waste is difficult to handle. On the other hand, the low selectivity, caused by the opening of the oxirane ring, leads to several by-products which decreases the process efficiency and increases the costs of the separation processes [3, 22, 23].

Various homogeneous catalysts have been proposed for this reaction, ranging from the use of enzymes to epoxidation

in the presence of polyoxometalates or coordination complexes. [3, 24–30]. From these studies it was observed that catalysts based on active transition metal centers such as Ru, Co, Mo, Rh, and Ti showed a high reactivity using more environmental friendly oxidizing agents such as O_2, H_2O_2, and TBHP [31–34]. Despite these advances, the problems associated with the recovery of the catalyst from the reaction medium, urged to examine heterogeneous catalysts such as ion exchange resins, clays, silicates, and inorganic oxides [3, 35–38]. Moreover, the incorporation of successful homogeneous catalysts on the surface of other inorganic solids have also been examined [39–41]. In the epoxidation of soybean oil, different heterogeneous catalysts have been evaluated, such as the Amberlite-16 resin, which was able to achieve a selectivity close to 80% or a natural zeolite with a selectivity of 82% and conversion of 96%, but using performic acid and H_2O_2 with formic acid, respectively [42, 43].

In the specific case of molybdenum, it represents one of the most studied structures in selective oxidation processes using enzymes known as oxotransferases, in which the active dioxomolybdenum ($Mo^{VI}O_2$) unit is involved in the oxygen atoms transfer processes [44–47]. Adapting these natural systems into analogous bio-inspired solid materials, $Mo^{VI}O_2$ active units have been incorporated into different supports such as TiO_2, SiO_2, and montmorillonite K10 through functional groups present on the ligands of their respective complexes. The obtained materials demonstrated to be highly selective in the oxidation of arylalkanes and epoxidation of both linear and cyclic alkenes. Moreover, their advantage of easy separation and reuse afterwards showed significant improvements in the conversion and selectivity compared to bulk catalysts doped or modified with transition metals [48–53].

Metal–organic frameworks better known as MOFs consist of metals linked systematically by organic ligands with suitable substituents [54, 55]. These alternating metal–ligand combinations result into highly crystalline solids with a defined topology, large internal surfaces that give rise to high specific surface areas (up to 7000 $m^2\ g^{-1}$), low densities (up to 0.13 $g\text{-}cm^{-3}$), and high metal content [56–61]. Additionally, the structural stability of the metal–organic framework and the functionality of the functional groups or heteroatoms present on the organic linker have been used for the post-synthetic functionalization of these materials with metals, or with catalytic centers [62, 63]. MOFs have been examined for a range of applications *e.g.* in the removal of pollutants [64–66], catalytic and photocatalytic coupling reactions [67–69] and CO_2 cycloaddition with epoxides [70–72].

Regarding epoxidation reactions catalyzed by metal–organic structures, new solid materials are reported every day, but their applications are restricted to low molecular weight unsaturated model molecules [55]. The novelty of this work was to evaluate the activity and stability of a metal–organic framework as a heterogenous catalyst in the epoxidation of unsaturated natural molecules with high molecular weight, which are of great industrial interest due to cheap and its availability as a renewable natural resource in Colombia and Latin-America. More specifically, it was examined the catalytic performance of the MoO_2 catalytic sites incorporated in a metal–organic structure denoted as MoO_2Cl_2@COMOC-4, in the soybean oil epoxidation. Currently, different methods and catalysts are being studied to obtain epoxidized vegetable oils (EVO), seeking to replace highly harmful chemical agents and move towards more ecological and environmentally friendly processes [73–76]. To the best of our knowledge, this previously reported metal–organic framework functionalized with dioxo-molybdenum (VI) active center [77] represents the first example of this type of porous solids applied in the epoxidation of vegetable oils, resulting in an alternative oxidation catalyst with an enhanced selectivity. Moreover, compared to the conventional vegetable oil oxidation methods, the proposed method is also much greener than other processes.

2 Experimental

All the experiments were performed using standard Schlenk techniques under an inert atmosphere. Scanning electron microscopy (SEM) images and energy-dispersive X-ray spectra (EDX) were obtained using a microscope FEI Quanta 200. Before analyses, the samples were metalized with a gold–palladium alloy using a Quorum Q150R ES metallizer. The surface area and porosity were determined from nitrogen (N_2) gas adsorption isotherms, taken at 77 K with a Micromeretics ASAP 2010 adsorption analyzer in the P/P_0 range of 1×10^{-5} to 0.99. Prior to the analyses, the solids were outgassed during 8 h at 110 °C and 1 µtorr. X-ray powder diffraction (XRPD) analyses were carried out using an X'Pert Pro MPD PANalytical equipment with Cu anode (Cu Kα radiation, $\lambda = 1.54056$ Å) and Bragg–Brentano configuration. The FT-IR ATR spectra were obtained using a Shimadzu IR prestige 21 spectrophotometer (Columbia, MD, USA). Diffuse reflectance UV–Vis spectra were recorded on a Hitachi U-3000 UV–Vis spectrophotometer. X-ray fluorescence (XRF) measurements were recorded with a NEX CG from Rigaku using a Mo-X-ray source. Differential Scanning Calorimetry (DSC) and Thermogravimetric analysis (TGA) was carried out using a Mettler Toledo Model TGA-1 thermal analyzer in a temperature range of 30–900 °C, under N_2 at a heating rate of 10 °C min^{-1}. A Bruker Avance 400 spectrometer was employed to measure the ^1H NMR spectra of the collected samples (60 mg) during catalytic experiments. The samples were dissolved in

deuterated chloroform (0.6 mL) containing TMS as internal standard.

2.1 Synthesis of COMOC-4

The synthesis of COMOC-4 was optimized at the gram scale based on a initially published procedure [61, 78]. $Ga(NO_3)_3{\cdot}H_2O$ (1.2 g, 4.4 mmol) and 2,2'bipyridene-5,5'-dicarboxylic acid (H2bpydc, 1.2 g, 5 mmol) were added to 120 mL of DMF in a 250 mL Schlenk flask equipped with a magnetic stirrer. The mixture was heated to 110 °C and kept at this temperature for 0.5 h. Afterwards, the mixture was heated to 150 °C and held at this temperature for 48 h under gentle stirring. At the end of the reaction, an orange powder was separated by filtration and washed thoroughly with DMF, methanol, and acetone. In the following step, the as-synthesized MOF was suspended in DMF (0.5 g in 50 mL DMF) and heated at 80 °C for 2 h after which it was collected through filtration, washed with DMF and acetone, and dried under vacuum.

3 Synthesis of MoO_2Cl_2@COMOC-4

MoO_2Cl_2@COMOC-4 was synthesized according to the previously published procedure [77]. Typically, 1.8 g MoO_2Cl_2 was added to 75.0 mL of THF and stirred for 10 min at room temperature. The yellowish solution was filtrated to remove the solid impurities and evaporated up to dryness to obtain the MoO_2Cl_2 $(THF)_2$ complex. The obtained complex was dissolved in 100 mL of THF, after which 2.5 g COMOC-4 was added to this solution and vigorously stirred at room temperature for 2 h. The solid product was filtered, washed with acetone, and activated before use.

3.1 Soybean Oil Epoxidation

The catalytic tests were carried out in a 25.0 mL round bottom flask equipped with a reflux condenser containing 1.0 g of soybean oil (1.0 mmol, equivalent to 4.0 mmol of double bonds), 10.0 mL of toluene, 66.0 mg of MoO_2Cl_2@COMOC-4 (0.04 mmol of Mo, equivalent to 1% of the double bonds present in oil), and a 70% TBHP in aqueous solution used as the oxidizing agent. Several reaction parameters were examined including the substrate/TBHP ratio and the temperature. At the end of the required reaction time, the mixture was filtered, and the catalyst was separated and washed (initially with toluene and then with acetone to be dried under vacuum). Before reuse and respective characterization of the catalyst, the solid was left under stirring in toluene at room temperature for 12 h after which it was filtered and dried under vacuum at 110 °C for 4 h. Consequently, the reaction mixture was subjected to a liquid–liquid extraction with 4.0% saline solution (15.0 mL×2) and 15.0% w/v sodium bisulfite solution (0.5 mL), in order to decompose the remaining oxidizing agent and remove its by-products (tert-butyl alcohol), from the reaction mixture. After that the organic phase was separated, dried over anhydrous Na_2SO_4, and the solvent was removed by rotaevaporation to obtain an off-white viscous liquid.

3.2 Analytical Quantification Methods

The monitoring of the epoxidation reaction was carried out by determination of the oxirane oxygen content (% O.O, expressed as grams of oxirane oxygen per 100 g of oil) and the iodine number (IY) (defined as g I_2 per 100 g of oil) before and after each catalytic test. The I.Y was determined by the classical method of Wijs [79], while the % O.O was calculated by applying the AOCS Official Method CD 9–57 [80]. The catalytic activity was evaluated by determination of the conversion, selectivity, and yield of the epoxidation reaction, using the following equations, where *i* and *f* represent initial and final values respectively:

$$\%Conversion = \frac{moles\,C = Cconsumed}{moles(C = C)_i}\text{x}100 = \frac{(I.Y)_i - (I.Y)_f}{(I.Y)_i}x100$$

$$\%Selectivity = \frac{moles\,C = C\,converted\,to\,epoxide}{moles\,de\,C = C\,consumed}x100$$

$$\%Epoxidation = \frac{moles\,C = C\,converted\,to\,epoxide}{(I.Y)_i}x100$$

The previously described catalytic activity parameters were validated by applying a second quantification method previously published using ^{1}H NMR in $CDCl_3$ [81]. The molecular weight (M) of the original soybean oil (equal to 871.5 g-mol^{-1}) was calculated from its ^{1}H NMR spectrum (Fig. 1), using the following equation:

$$M = \frac{15.034\boldsymbol{G}}{3NF} + \frac{14.026(C + D + E + F + H}{2NF} + \frac{26.016(A - NF)}{2NF} + 173.1,$$

where NF is the normalization factor (the relative peak area of one hydrogen) calculated from the signal area associated with the four hydrogens of the methylene groups of the glycerol moiety (signal B in Fig. 1).

The number of double bonds (ND) present in the initial soybean oil sample was determined by the following equation:

$$ND_i = \frac{A - NF}{2NF}$$

which was used to determine the percentage of conversion, epoxidation, and selectivity according to [82]:

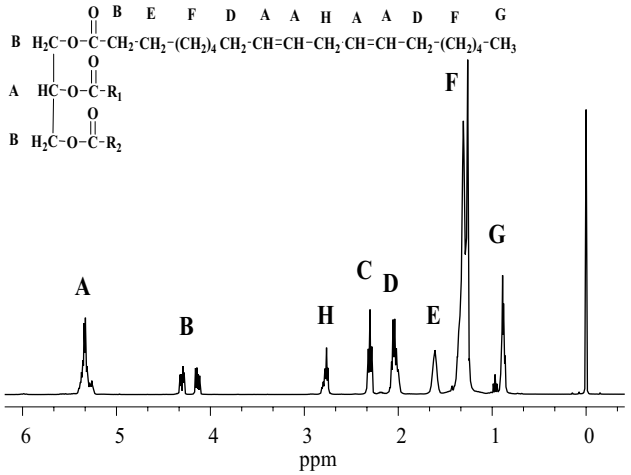

Fig. 1 ^{1}H NMR spectrum of the soybean oil sample represented by a triglyceride of linoleic acid (R_1 and R_2 are alkyl groups)

$$\%Conversion = \frac{ND_i - ND_f}{ND_i} x100,$$

$$\%Epoxidation = \frac{(K+L)/2}{NF \times ND_i} x100,$$

$$\%Selectivity = \frac{\%Epoxidation}{\%Conversion} x100,$$

where ND_f is the number of double bonds that remain unreacted and K and L are the peak areas associated with the hydrogens of the epoxide groups that are identified by new signals at chemical shifts of 2.9 (monoepoxide) and 3.1 (diepoxide) ppm, respectively.

4 Results and Discussion

4.1 Synthesis, Characterization, and Structural Information

The X-ray diffraction analysis of COMOC-4 confirmed its crystallinity which corresponds to an open architecture typically observed for MIL-47 and MIL-53 series but constructed by infinite chains of octahedral $GaO_4(OH)_2$ units, in which each Ga^{3+} ion is bound to four dicarboxy-bipyridine ligands and two μ_2-trans hydroxide anions (Fig. 2).

After incorporation of MoO_2Cl_2, the main Bragg diffraction angles of COMOC-4 are preserved, but a slight decrease in the intensities of some peaks in the MoO_2Cl_2@COMOC-4 diffractogram was observed, suggesting that the crystallinity of the COMOC structure might be partially impaired in the post-functionalization process [83]. Additionally, new

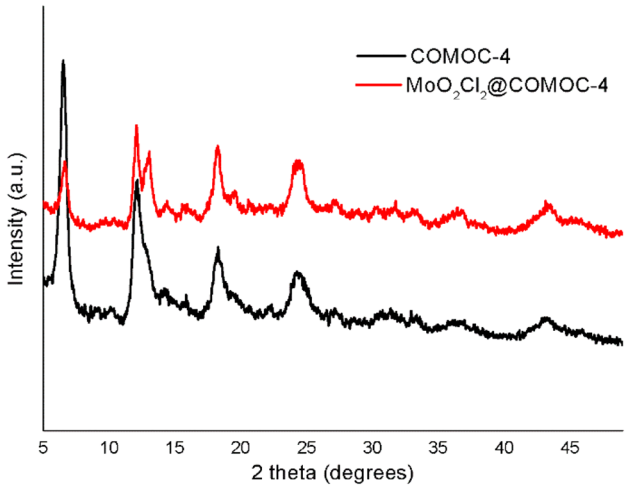

Fig. 2 XRPD patterns of COMOC-4 and MoO_2Cl_2@COMOC-4

Bragg reflections (or splitting) have been identified close to the original ones at of lower intensity, originated by slight distortions in the shape and angle of the linkers because of the interaction between the Mo(VI) center and the chelating nitrogen atoms (about $2\theta = 14°$). The results obtained from nitrogen adsorption, infrared and UV–Vis diffuse reflectance spectroscopy for COMOC-4 and MoO_2Cl_2@COMOC-4 are in agreement with the previously reported data (see Supporting information, Figure S1-S4 and Table S1). BET surface areas and pore volumes are 742 m^2/g and 1.66 cm^3/g for COMOC-4 and 214 m^2/g and 0.78 cm^3/g for MoO_2Cl_2@COMOC-4, reveling a partial deterioration of the textural properties as consequence of the incorporation of MoO_2Cl_2 units. A quantity of 5.9% Mo in the MoO_2Cl_2@COMOC-4 sample was determined by means of XRF. In other words, 22% of bipyridine sites was loaded with the active dioxomolybdenum (VI) complex (the Mo/Ga molar ratio is 0.22) based on the empirical formula of the catalysts, namely $C_{12}H_7N_2Cl_{0.44}GaMo_{0.22}O_{4.44}$.

4.2 Soybean Oil Epoxidation Reaction

The catalytic performance of the MoO_2Cl_2@COMOC-4 catalyst was evaluated in the epoxidation of soybean oil using TBHP as oxygen donor agent. In the experimental design, the molar concentration of the oil (≈0.1 M) and the molar relation between the number of unsaturations and Mo active centers were kept constant (100:1), using toluene as solvent. To demonstrate the participation of the MoO_2 active center and the role of the oxidizing agent in the catalytic epoxidation process, different control experiments were carried out. An initial control reaction was performed at 80 °C in the presence of MoO_2Cl_2@COMOC-4 and in the absence of the oxygen donor agent (TBHP). A conversion of 3.3% and a selectivity of 17.7% (Table 1, Entry 1) were obtained, due

Table 1 Results of the preliminary experiments of epoxidation of soybean oil at 80 °C

Entry	Temperature (°C)	Reaction time (h)	Conversion (%)	Epoxidation (%)	Selectivity (%)	TON[d]	TOF (h^{-1})[e]
1[a]	80	4	3.3	0.6	17.7	0.5	0.1
2[b]	80	4	37.7	5.0	13.3	–	–
3[c]	80	4	17.0	9.6	56.4	9.4	2.3

[a]Reaction was carried out with toluene as solvent and molar ratio of TBHP:number of double bonds in the oil:catalyst of 0:100:1

[b]Reaction was carried out with toluene as solvent and molar ratio of TBHP:number of double bonds in the oil:catalyst of 100:100:0

[c]Reaction was carried out with toluene as solvent and molar ratio of TBHP:number of double bonds in the oil:catalyst of 100:100:1

[d]*TON* total turnover number, moles of epoxide formed per mole of catalyst

[e]*TOF* turnover frequency which is calculated by the expression (epoxide)/(catalyst) × time (h^{-1})

to the oxygen atom transfer from the dioxo-molybdenum (VI) unit towards the double bond [48, 84–86]. A scheme of the stoichiometric epoxidation process of soybean oil from MoO_2Cl_2@COMOC-4 catalyst without oxygen donor agent is presented in Fig. 3.

A second control reaction using the same temperature was carried out with TBHP as oxygen donor agent using a molar ratio TBHP: double bonds: catalyst of 100:100:0 (without Mo catalyst). In this test, a conversion of 37.7% of the respective oil was observed but with a very low selectivity (13.3%) towards the epoxide (Table 1, Entry 2). This low selectivity is caused by side reactions that result in different products such as alcohols, ketones, or carboxylic derivates (Fig. 4), which is the main problem associated with conventional epoxidation methods [3].

A first test in the presence of MoO_2Cl_2@COMOC-4 and the oxygen donor agent (TBHP) was carried out at 80 °C during 4 h employing a molar ratio TBHP: double bonds: catalyst of 100:100:1. As shown in Table 1, entry 3, a conversion of 17.0% and a selectivity of 56.4% were obtained. The respective monitoring of the oil sample, before and at the end of the reaction, using ^{1}H NMR spectroscopy corroborated the appearance of the oxirane ring (signals at 3.1 and 2.9 ppm) and the respective decrease in the signal corresponding to the proton A, as seen in Fig. 5. A preference towards the formation of monoepoxide was deduced because of the higher intensity of the signal at 2.9 ppm compared to the characteristic diepoxide signal at 3.1 ppm [87].

It is well known that transition metal ions in their highest oxidation state such as Mo(VI) can simultaneously support one or several oxygen ligands such as oxo, peroxide, hydroxide or hydroperoxide in their coordination sphere, and the type of oxygen ligand that is incorporated into the active molybdenum center depends on the oxidizing agent used in the respective catalytic process [85, 86]. On the other hand, although the mechanism of epoxidation of alkenes is still controversially discussed [84, 88, 89], the epoxidation mechanism in vegetable oils using THBP as an oxidizing agent has been previously reported [90], and the results are in agreement with the ideas proposed by Sobczak [29], that begins with the formation of the species

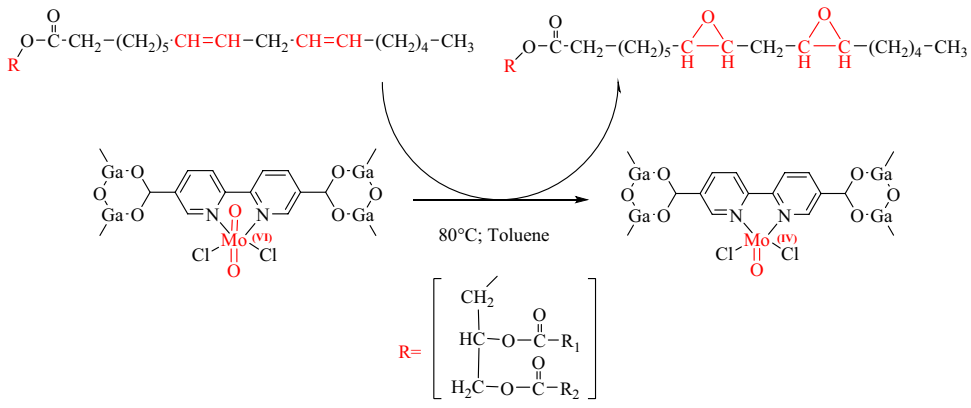

Fig. 3 Stoichiometric epoxidation of soybean oil from MoO_2Cl_2@COMOC-4 catalyst without oxygen donor agent. No reaction products were obtained when COMOC-4 solid was evaluated under the same conditions

Fig. 4 Scheme of some side reactions under different conditions in soybean oil epoxidation process

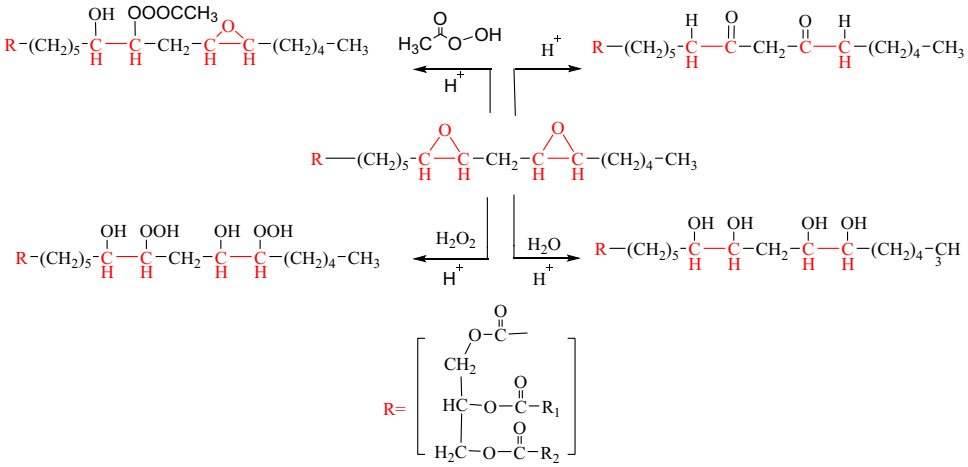

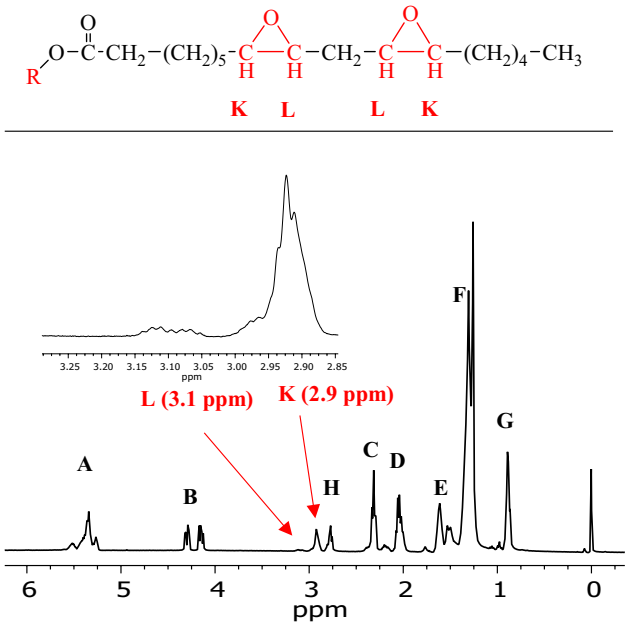

Fig. 5 ^{1}H NMR spectrum of soybean oil after epoxidation reaction

Mo(VI)–O–O–$(CH_3)_3$ as an intermediary through coordination via the peroxo oxygen bonded to the molybdenum atom, and formation of a hydrogen bonding with one of the terminal oxygens. The metal center acts as a Lewis acid by removing charge from the O–O bond, facilitating its dissociation, combined it with the olefin nucleophilic attack to the electrophilic oxygen atom of the coordinated peroxide (Fig. 6) [91, 92].

To evaluate the stability of the MoO_2Cl_2@COMOC-4 catalyst during the soybean oil epoxidation reaction, the used catalyst was characterized by means of XRPD, IR spectroscopy, thermogravimetric analyses, and SEM microscopy (Figs. 7 and 8).

XRPD analyses of the used catalyst corroborated the structural integrity of the support in the soybean epoxidation reaction (see Fig. 7a), and the IR spectrum of the catalyst after reaction (Fig. 7b) has the same signals in the range 600–1800 cm^{-1} assigned to the stretching vibrations of the bipyridine ligand in the fresh MoO_2Cl_2@COMOC-4 catalyst. Furthermore, no changes in the intensity of the symmetric and asymmetric vibrations of dioxo-molybdenum (MoO_2) were observed in the region between 890 and 950 cm^{-1}, evidencing the preservation of the oxidation state in the metal center during the catalytic test. The thermogravimetric analyses, presented in Fig. 7c, demonstrate the high stability of the metal–organic structure since no significant changes in the loss of mass of the catalyst were observed between the fresh and spend catalyst. The temperature decomposition of the catalysts was determined by DSC [93] (Figure S5 -Supporting information) obtaining a value close to 500 °C for the fresh solid, which presented a slight decrease (around 8 °C) when compared to the used MoO_2Cl_2@COMOC-4 catalyst.

Finally, SEM images of the MoO_2Cl_2@COMOC-4 catalyst revealed heterogeneous morphology and particle sizes, and EDX analyses confirmed the presence of molybdenum in the metal–organic framework catalyst before and after the epoxidation process (Fig. 8). Evidently, irregular morphologies were observed for MoO_2Cl_2@COMOC-4 catalyst before and after used, but the particle size was decreased for the used solid. This fractionation is a consequence of the mechanical attrition of the catalyst throughout the catalytic process. From these initial results, it was proposed to examine the influence of concentration of the oxidizing agent, the reaction time, and the reaction temperature in the heterogenous soybean oil epoxidation catalyzed by the MoO_2Cl_2@COMOC-4 solid.

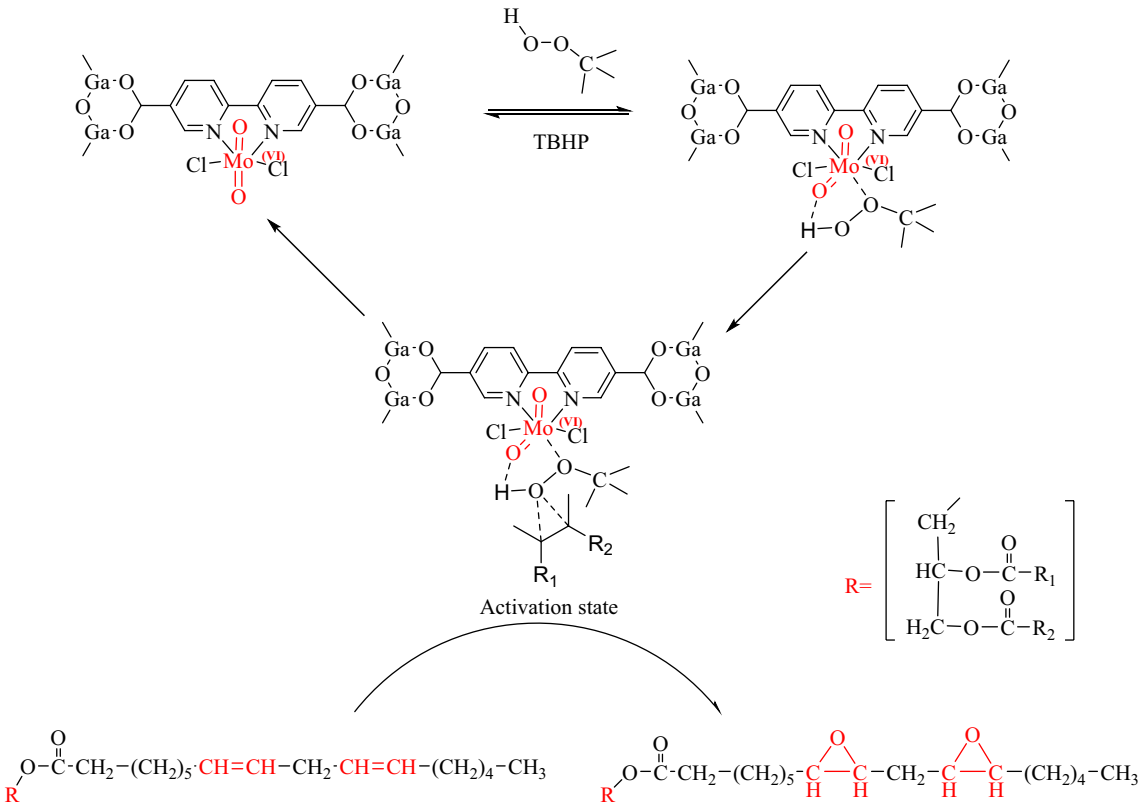

Fig. 6 Illustration of the soybean epoxidation reaction catalyzed by MoO_2Cl_2@COMOC-4 with hydroperoxides

4.3 Influence of the Concentration of Oxidizing Agent

To determine the optimal reaction conditions in the presence of the oxidizing agent (TBHP), three additional experiments were carried out in which the molar ratio of the oxidizing agent was varied with respect to the number of unsaturation contained in the oil (Fig. 9 and Table 2), while keeping the reaction time (4 h), the temperature (80 °C) and the moles of double bonds constant (Entries 2–4, Table 2). Initially, a 2:1 molar ratio of oxidizing agent: unsaturations was evaluated, which resulted in an increase in the conversion, selectivity, and percentage of epoxidation (Entry 2, Table 2).

Using an oxidizing agent:doble bond ratio to 4:1 resulted only in a slightly further increase in the selectivity percentage (Fig. 9, and Entry 3 of Table 2) while the conversion and percentage of epoxidation decreased. This is because the generated by-product tert-butanol interferes in the catalytic cycle, which becomes more evident in our case when an oxidizing agent:double bond ratio of 8:1 was used (Entry 4, Table 2). In other words, increasing the concentration of the oxidizing agent leads to its decomposition and formation of larger amounts of by-product (tert-butanol), which was subsequently detected through the purification processes.

4.4 Influence of Reaction Time

Once the best oxidizing agent:double bond molar ratio was determined at 80 °C, the influence of the reaction time was studied. Initially, two reaction times were evaluated, 4 and 24 h (Entry 2 and 5, Table 2). After 4 h of reaction, the conversion reached a value of 18.6%, while after 24 h a conversion of 75.8% was obtained (Fig. 10). Although a higher conversion was noted, the selectivity decreased from 66.6% to 14.8% after 24 h of reaction. This result shows that the epoxidation product is formed quite fast and that long reaction times favors the formation of by-products due to collateral reactions [94]. Additionally, a prolonged reaction time leads to a significant darkening (browning) of the oil after prolonged contact with atmospheric oxygen, which indicates the occurrence of undesired oxidation processes [95].

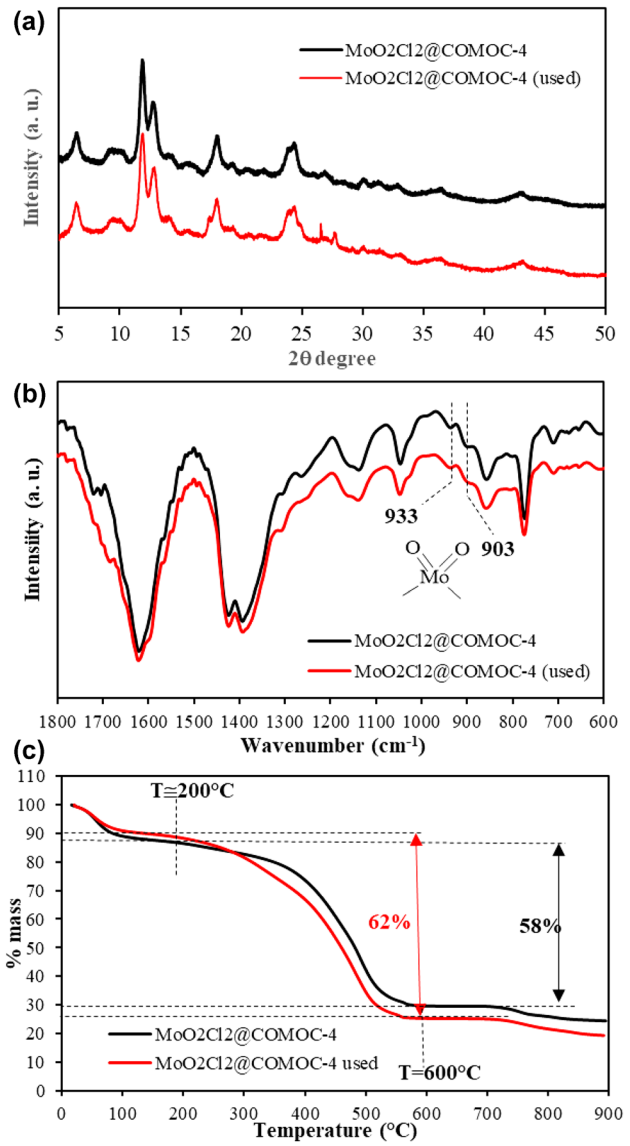

Fig. 7 XRPD, IR and thermogravimetric analysis of MoO_2Cl_2@COMOC-4 catalyst fresh and used in the epoxidation reaction with TBHP

4.5 Influence of Temperature

To evaluate the influence of the reaction temperature, two additional experiments were carried out (at room temperature and at 110 °C) during 4 h of reaction, using the optimal concentration of the oxidizing agent. The catalytic activity of MoO_2Cl_2@COMOC-4 with TBHP at room temperature showed no formation of reaction products. On the contrary, an increase of the temperature to 110 °C (Entry 6, Table 2) led to a significant increase in the reaction yield (26.6% epoxidation, 29.4% conversion, and 90.6% selectivity) compared to the results obtained at 80 °C (Entry 2), as evidenced in Fig. 11.

Such an increase in activity for the vegetable oil oxidation was already observed for different catalysts in literature. However, it is important to note that the conversion is relatively low compared to the oxidation of molecules such as cyclohexene, cyclooctene or small linear alkenes with this type of catalyst [57, 77]. This low conversion is probably the result of the larger size of the constituent molecules of soybean oil, restricting the entering of the molecules into the pores of MOF.

Finally, two more reactions were carried out to establish the optimal reaction time at 110 °C. The reactions carried out for 8 h and 2 h (Entries 7 and 8, Table 2) did not show better results than the reaction performed during 4 h of catalysis at the same temperature. In this way, a prolonged reaction time largely affects the selectivity of the reaction. Also, from the TON and TOF (26.1 and 6.5 h^{-1}) values, it is clear the catalyst exhibits its highest catalytic activity and selectivity after 4 h of reaction at 110 °C (Fig. 12).

Compared to published Mo-based heterogeneous and homogeneous catalyst systems (Entry 1–3), presented in Table 3, all these catalysts show more conversion than MoO_2Cl_2@COMOC-4 in epoxidation of soybean oil, reaching transformations of the aliphatic double bonds above 30%. The selectivity values observed, on the contrary, do show that the MoO_2 unit is more selective being directly functionalized onto the solid metal–organic structure. This phenomenon has been previously observed in epoxidation reactions of natural products such as Limonene and alpha-pinene, using different supports, and has been associated with the stability generated at the active center, when it is incorporated covalently on a solid structure, originating a more selective process towards the epoxide [102–104]. Additionally, when MoO_2Cl_2@COMOC-4 was compared with heterogeneous catalysts based on oxo-tungsten active centers (Entry 4–5, Table 3), SiO_2, Amberlite IR-120, or AlO_3 solid supports that use inorganic acids as co-catalysts (Entry 7–9, Table 3), the same trend was observed in the conversion and selectivity values. Finally, it is important to highlight that in our case, both the mass of catalyst used and the optimal reaction time are significantly lower than the heterogeneous processes that have shown good results in conversion and selectivity (Entry 6–10, Table 3), which may be favorable in economic terms in the future [105].

4.6 Catalytic Reuse Evaluation

To evaluate the reusability of the MoO_2Cl_2@COMOC-4 catalyst in the soybean oil epoxidation at 110 °C, the solid catalyst was separated from the reaction medium by means of filtration after 4 h of reaction, washed with toluene and

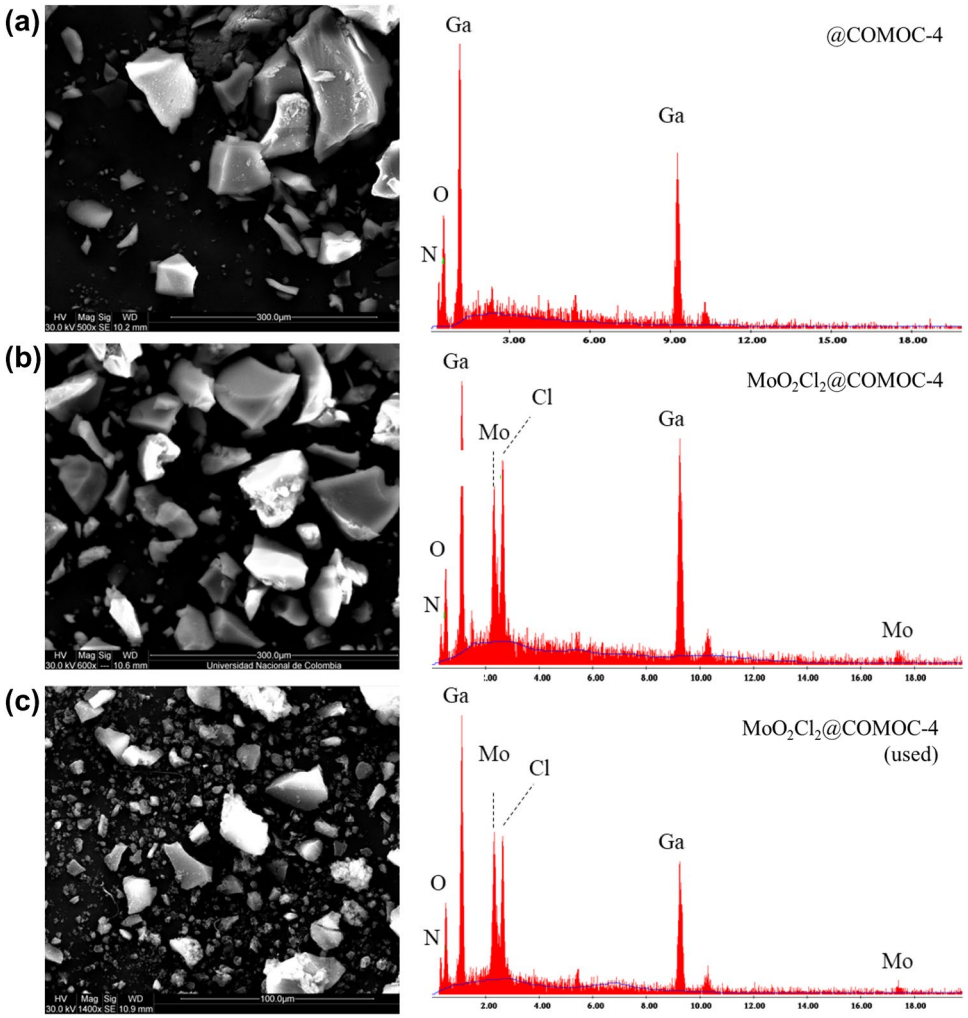

Fig. 8 SEM images and EDX of **a** COMOC-4, **b** MoO_2Cl_2@COMOC-4 catalyst, and **c** used MoO_2Cl_2@COMOC-4 catalyst

acetone, and dried in vacuum. Interestingly, as shown in Table 4, the catalytic activity is preserved during a new successive catalytic test with a slight decrease in the % conversion and % epoxidation (22.0% and 20.3% respectively), but an increase in the selectivity values reaching 92.3%.

Initially, to analyze the stability of the active center on the surface, an elemental analysis of Mo using Plasma Mass Spectrometry (ICP-MS) was carried out, evidencing a slow reduction of the concentration of active center (decrease 0.7% wt Mo), but confirming the presence of molybdenum in the metal–organic framework catalyst after the epoxidation process. The oxidation state stability of MoO_2 (VI) entity in MoO_2Cl_2@COMOC-4 catalyst was confirmed by XPS measurements before and after catalysis (Fig. 13). In both samples Mo is present in the oxidation state + 6, confirmed by the molybdenum 3d peak signals (Mo3d5/2 and

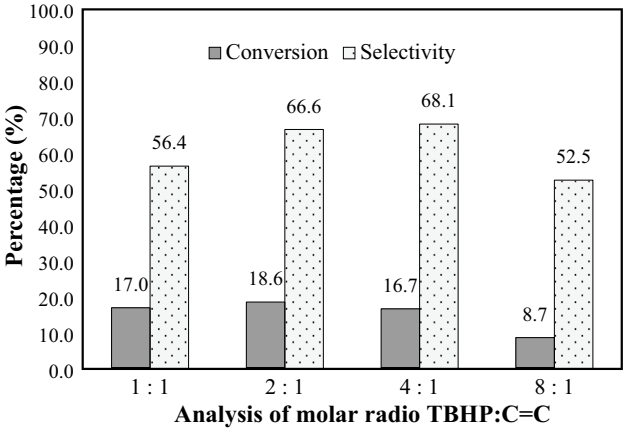

Fig. 9 Analysis of the molar ratio variation oxidizing agent: double bonds in soybean oil epoxidation at 80 °C catalyzed by MoO_2Cl_2@COMOC-4 with TBHP as an oxidizing agent

Table 2 Results obtained to determine the optimal reaction conditions in soybean oil epoxidation catalyzed by MoO_2Cl_2@COMOC-4 with TBHP as oxidizing agent

Entry	Temperature (°C)	Reaction time (h)	Conversion (%)	Selectivity (%)	Epoxidation (%)	TON[e]	TOF (h^{-1})[f]
1[a]	80	4	17.0	56.4	9.6	9.4	2.3
2[b]	80	4	18.6	66.6	12.4	12.1	3.0
3[c]	80	4	16.7	68.1	11.4	11.3	2.8
4[d]	80	4	8.7	52.5	4.6	6.9	1.7
5[b]	80	24	75.8	14.8	11.2	10.0	0.4
6[b]	110	4	29.4	90.6	26.6	26.1	6.5
7[b]	110	8	34.8	28.5	9.9	9.8	1.2
8[b]	110	2	18.3	78.6	14.4	14.3	7.2

[a]Molar ratio of TBHP: number of double bonds in the oil:catalyst of 100:100:1

[b]Molar ratio of TBHP: number of double bonds in the oil:catalyst of 200:100:1

[c]Molar ratio of TBHP: number of double bonds in the oil:catalyst of 400:100:1

[d]Molar ratio of TBHP: number of double bonds in the oil:catalyst of 800:100:1

[e]*TON* Total turnover number, moles of epoxide formed per mole of catalyst

[f]*TOF* Turnover frequency, which is calculated by the expression (epoxide)/(catalyst) × time (h^{-1})

Mo 3d3/2 Peaks) localized at an average value 232.4 and 235.6 eV, characteristics of this oxidation state [106].

Further, the surface properties of the metal–organic structure obtained by N_2 adsorption–desorption measurements of the new and used catalyst were compared. Evidently, the N_2 adsorption–desorption isotherms of MoO_2Cl_2@COMOC-4 fresh and used are different (Fig. 14), revealing a decrease in the BET surface area and porosity. Adsorption–desorption isotherms type IVa (IUPAC classification), typical of mesoporous materials, was maintained. The BJH pore size distributions (Fig. 14-inset) show monomodal functions with pore diameters centered about 14 nm and 12 nm for the catalysts fresh and used, respectively. However, the population of pores (cumulative pore volume) was clearly reduced for the used catalyst. Furthermore, values of BET area and pore volume of 214 m^2/g and 0.78 cm^3/g for fresh MoO_2Cl_2@COMOC-4, and 73 m^2/g and 0.31 cm^3/g for used MoO_2Cl_2@COMOC-4, were obtained (Table 5). These reductions of porosity and surface areas likely are the result of the partial blockage of the pores by the large molecules of vegetable oil, which is understandable considering the oleic nature and bulky size of oleic and linoleic acid (main constituents of the vegetable oil under study). A similar effect has been previously observed by other authors [83]. These reductions of porosity and surface area and this low conversion are probably the result of the size of the constituent molecules of soybean oil, restricting the entering of the molecules into the pores of MOF, suggesting that the reaction takes place mainly on the active sites available on the

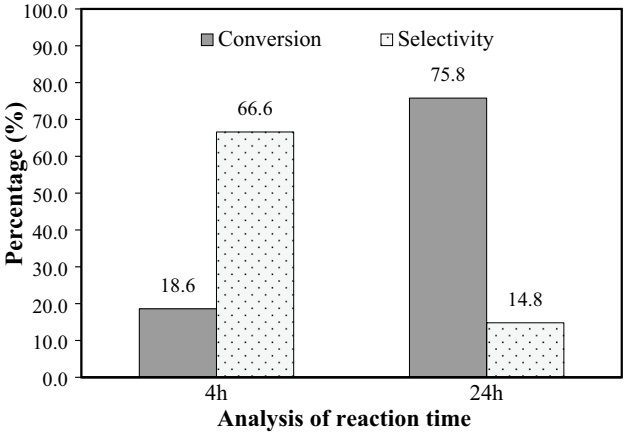

Fig. 10 Evaluation of the reaction time in the soybean oil epoxidation at 80 °C catalyzed by MoO_2Cl_2@COMOC-4 with TBHP

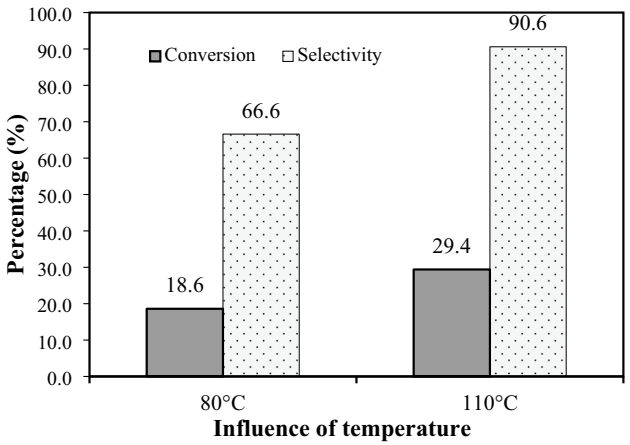

Fig. 11 Evaluation of the reaction temperature in the soybean oil epoxidation at 4 h of reaction catalyzed by MoO_2Cl_2@COMOC-4 with TBHP

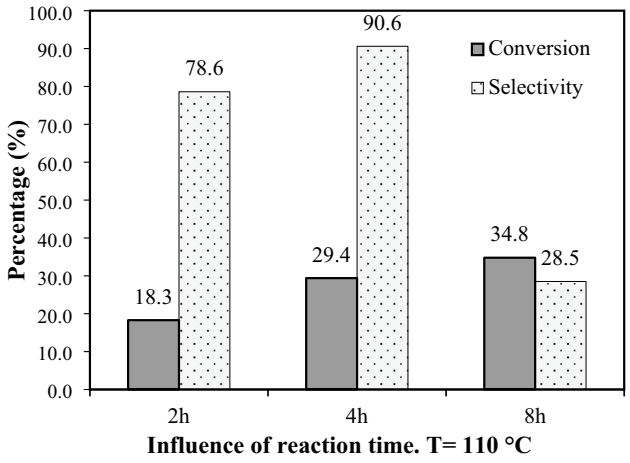

Fig. 12 Evaluation of the reaction time for the soybean oil epoxidation at 110 °C catalyzed by MoO_2Cl_2@COMOC-4 with TBHP

surface of the catalyst. The results suggest that MoO_2Cl_2@COMOC-4 has good potential to be reusable catalysis for the epoxidation processes of vegetable oils; nevertheless, more research is necessary to diminish or reduce the effect of pores clogging.

5 Conclusions

The catalytic activity of MoO_2Cl_2@COMOC-4 was demonstrated in the selective epoxidation of commercial soybean oil in the presence of tert-butyl-hydroperoxide as an oxidizing agent. The analysis of the temperature, the reaction time, and the TBHP: double bonds molar ratio in the oil revealed that the best conversion, selectivity, and epoxidation results were obtained at 110 °C for 4 h and a 200: 100: 1 molar ratio (TBHP: double bonds: catalyst).

Table 3 Comparison of catalytic activity of MoO_2Cl_2@COMOC-4 with other heterogeneous catalysts in the soybeam oil epoxidation

Entry	Catalyst	Oxidant	Oxidant to substrate molar ratio	catalyst mass (g)	Time (h)	T (°C)	Conversion/Selectivity	References
1	$[MoO_2(acac)_2]$	TBHP	1.0	0.013	24	80	94.1/ 41.4[a]	[87]
2	$[MoO_2(acac)_2]$-montmorillonite K-10	TBHP	2.0	0.480	24	80	65.0/24.8	[51]
3	MoO_3/Al_2O_3	TBHP	1.4	0.300	4	80	36.3/34.0	[96]
4	$\{PO_4[W(O)(O_2)_2]_4\}^3$-Halloysite nanotubes	H_2O_2	3.0	0.300	2.6	40	22.3/55.0[b]	[97]
5	$\{PO_4[W(O)(O_2)_2]_4\}^{3-}$ entrapped into SBA-15	H_2O_2	5.0	2.000	5	70	55.7/68.2	[98]
6	Cadmium/titanium silicalite-1 zeolite	H_2O_2	2.5	0.100	12	80	17.8/98[c]	[99]
7	Amberlite IR-120	TBHP	2.2	0.200	5	80	82.6/82.3	[100]
8	Meso-Ti-HMS	TBHP	1.1	0.500	24	80	72.0/50.0	[23]
9	γ-Al_2O_3	H_2O_2	5.0	0.600	10	80	75.0/64.0[d]	[75]
10	SnO_2-Al_2O_3-NiO/SO_4^{2-}	H_2O_2/HCOOH	2.0/2.0	3.0 (0.5%wt)	1.5	65	86.97%[e]	[101]
11	MoO_2Cl_2@COMOC-4	TBHP	2.0	0.066	24	110	29.4/90.6	This work

[a]Catalyst in homogeneous phase

[b]Mechanical agitation combining with ultrasonic agitation

[c]The fresh catalyst has lost its activity after one use, although the activity can be recovered by calcination at high temperature

[d]In the presence of inorganic acids such as acetic acid

[e]Relative conversion to oxirane

Table 4 Results of the catalyst reuse evaluation in soybean oil epoxidation catalyzed by MoO_2Cl_2@COMOC-4 with TBHP as oxidizing agent a 110 °C

	Conversion[a] (%)	Selectivity (%)	Epoxidation (%)	TON [b]	TOF (h^{-1}) [c]
Run 1	29.4	90.6	26.6	26.1	6.5
Run 2	22.0	92.3	20.3	23.4	5.8

[a]Molar ratio of TBHP: number of double bonds in the oil:catalyst of 200:100:1. Reaction time: 4 h

[b]*TON* Total turnover number, moles of epoxide formed per mole of catalyst

[c]*TOF* Turnover frequency, it was calculated by the expression (epoxide)/(catalyst) × time (h^{-1})

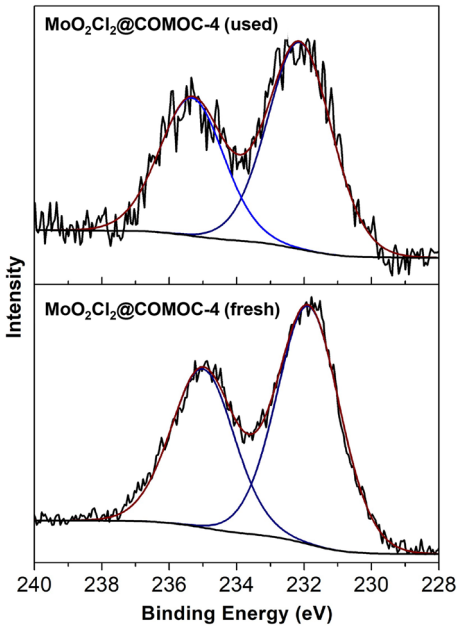

Fig. 13 The Mo 3d3/2 and Mo 3d5/2 peak of MoO_2Cl_2@COMOC-4 catalyst before and after catalysis

The results obtained from the stability of the catalyst during two cycles confirmed the catalyst's ability to be reused in catalytic processes for the recovery of vegetable oils.

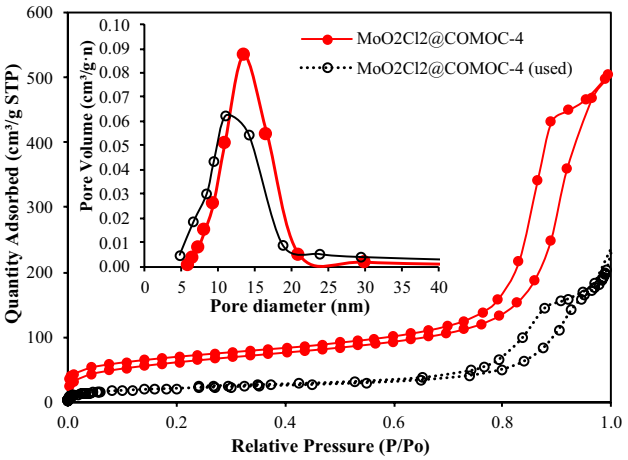

Fig. 14 Nitrogen adsorption/desorption isotherm and pore size distribution analysis (inset) of MoO_2Cl_2@COMOC-4 catalyst before and after catalysis

Table 5 Results of the Mo loading, surface area and pore size distribution of MoO_2Cl_2@COMOC-4 catalyst before and after catalysis

Catalysts	Mo loading % wt[a]	Lagmuir Surface Area (m^2/g)	BET Surface Area (m^2/g)	Pore Volume (cm^3/g)[b]
MoO_2Cl_2@COMOC-4	5.8	419	214	0.78
MoO_2Cl_2@COMOC-4 (used)	5.1	66	73	0.31

[a]Determined using plasma mass spectrometry (ICP-MS)

[b]Pore volume determined by Gurvitsch´s method at $P/P_0 = 0.99$

Supplementary Information The online version contains supplementary material available at https://doi.org/10.1007/s10562-022-04096-y.

Acknowledgements This work was financially supported by the Universidad Nacional de Colombia and the Faculty of Sciences of Universidad Nacional de Colombia by the internal Project code 37526. NJC appreciates the collaboration of the Professor Freddy A. Ramos from the UNAL-NMR laboratory for his support in the quantification of the reaction products.

Author Contributions Diana C. Martínez R.: Data curation, Investigation, Formal analysis, Methodology, Visualization, Writing—review & editing, CAT Formal analysis, Investigation, Supervision, Validation, Writing—review & editing, JGC: Formal analysis, Investigation, Supervision, Validation, Writing—review & editing, NJC: Conceptualization, Experimental plan, Formal analysis, Funding acquisition. Validation, Writing—original draft.

Funding Open Access funding provided by Colombia Consortium. This work was financially supported by the Universidad Nacional de Colombia and the Faculty of Science through the internal Project (Grant No. 37526).

Data Availability The spectroscopic measurements were kept in their original files. The quality and reproducibility of the catalytic experiments were verified by triplicate analysis and the results reported in this manuscript correspond to the average of these measurements. For the reported synthesis procedure, no details were omitted for obtaining these materials as they are reported in this article. In general, data were acquired by standard scientific procedures employed in the fields of solid-state chemistry, analytical chemistry, and physical chemistry. All experiments are reproducible and reliable.

Code Availability Not applicable.

Declarations

Conflict of interest There are no conflicts to declare.

References

1. Meier MAR, Metzger JO, Schubert US (2007) Plant oil renewable resources as green alternatives in polymer science. Chem Soc Rev 36:1788–1802. https://doi.org/10.1039/b703294c
2. Biermann U, Bornscheuer U, Meier MAR et al (2011) Oils and fats as renewable raw materials in chemistry. Angew Chemie—Int Ed 50:3854–3871. https://doi.org/10.1002/anie.201002767
3. Danov SM, Kazantsev OA, Esipovich AL et al (2017) Recent advances in the field of selective epoxidation of vegetable oils and their derivatives: a review and perspective. Catal Sci Technol 7:3659–3675. https://doi.org/10.1039/c7cy00988g
4. Gallezot P (2012) Conversion of biomass to selected chemical products. Chem Soc Rev 41:1538–1558
5. Faba L, Díaz E, Ordóñez S (2015) Recent developments on the catalytic technologies for the transformation of biomass into biofuels: a patent survey. Renew Sustain Energy Rev 51:273–287. https://doi.org/10.1016/j.rser.2015.06.020
6. Corma Canos A, Iborra S, Velty A (2007) Chemical routes for the transformation of biomass into chemicals. Chem Rev 107:2411–2502. https://doi.org/10.1021/cr050989d
7. Knothe G (2012) Vegetable oils. Handb Bioenergy Crop Plants 793–810. https://doi.org/10.32741/fihb.19.vegetableoil
8. Gunstone FD (2011) Vegetable Oils in Food Technology: Composition, Properties and Uses, Second Edition, Wiley-Blackwell, Oxford, UK
9. Barnwal BK, Sharma MP (2005) Prospects of biodiesel production from vegetable oils in India. Renew Sustain Energy Rev 9:363–378. https://doi.org/10.1016/j.rser.2004.05.007
10. Issariyakul T, Dalai AK (2014) Biodiesel from vegetable oils. Renew Sustain Energy Rev 31:446–471. https://doi.org/10.1016/j.rser.2013.11.001
11. Javni I, Petrović ZS, Guo A, Fuller R (2000) Thermal stability of polyurethanes based on vegetable oils. J Appl Polym Sci 77:1723–1734. https://doi.org/10.1002/1097-4628(20000822)77:8<1723::AID-APP9>3.0.CO;2-K
12. Sawpan MA (2018) Polyurethanes from vegetable oils and applications: a review. J Polym Res. https://doi.org/10.1007/s10965-018-1578-3
13. Guo A, Zhang W, Petrovic ZS (2006) Structure-property relationships in polyurethanes derived from soybean oil. J Mater Sci 41:4914–4920. https://doi.org/10.1007/s10853-006-0310-6
14. Zhang C, Garrison TF, Madbouly SA, Kessler MR (2017) Recent advances in vegetable oil-based polymers and their composites. Elsevier B.V.
15. Hosney H, Nadiem B, Ashour I et al (2018) Epoxidized vegetable oil and bio-based materials as PVC plasticizer. J Appl Polym Sci 135:1–12. https://doi.org/10.1002/app.46270
16. Karmalm P, Hjertberg T, Jansson A, Dahl R (2009) Thermal stability of poly(vinyl chloride) with epoxidised soybean oil as primary plasticizer. Polym Degrad Stab 94:2275–2281. https://doi.org/10.1016/j.polymdegradstab.2009.07.019
17. Nihul PG, Mhaske ST, Shertukde VV (2014) Epoxidized rice bran oil (ERBO) as a plasticizer for poly(vinyl chloride) (PVC). Iran Polym J 23:599–608. https://doi.org/10.1007/s13726-014-0254-7
18. He W, Zhu G, Gao Y et al (2020) Green plasticizers derived from epoxidized soybean oil for poly (vinyl chloride): continuous synthesis and evaluation in PVC films. Chem Eng J 380:122532. https://doi.org/10.1016/j.cej.2019.122532
19. Erhan SZ, Asadauskas S (2000) Lubricant basestocks from vegetable oils. Ind Crops Prod 11:277–282. https://doi.org/10.1016/S0926-6690(99)00061-8
20. Wagner H, Luther R, Mang T (2001) Lubricant base fluids based on renewable raw materials: their catalytic manufacture and modification. Appl Catal A Gen 221:429–442. https://doi.org/10.1016/S0926-860X(01)00891-2
21. Prileschajew N (1909) Oxydation ungesättigter verbindungen mittels organischer Superoxyde. Berichte der Dtsch Chem Gesellschaft 42:4811–4815. https://doi.org/10.1002/cber.190904204100
22. Mungroo R, Pradhan NC, Goud VV, Dalai AK (2008) Epoxidation of canola oil with hydrogen peroxide catalyzed by acidic ion exchange resin. JAOCS, J Am Oil Chem Soc 85:887–896. https://doi.org/10.1007/s11746-008-1277-z
23. Campanella A, Baltanás MA, Capel-Sánchez MC et al (2004) Soybean oil epoxidation with hydrogen peroxide using an amorphous Ti/SiO_2 catalyst. Green Chem 6:330–334. https://doi.org/10.1039/B404975F
24. Zhang X, Burchell J, Mosier NS (2018) Enzymatic Epoxidation of High Oleic Soybean Oil. ACS Sustain Chem Eng 6(7):8578–8583. https://doi.org/10.1021/acssuschemeng.8b00884
25. Gerbase AE, Gregório JR, Martinelli M et al (2002) Epoxidation of soybean oil by the methyltrioxorhenium-CH_2Cl_2/H_2O_2

catalytic biphasic system. J Am Oil Chem Soc 79:179–181. https://doi.org/10.1007/s11746-002-0455-0
26. Chen Z, Yin G (2015) The reactivity of the active metal oxo and hydroxo intermediates and their implications in oxidations. Chem Soc Rev 44:1083–1100. https://doi.org/10.1039/C4CS00244J
27. Joergensen KA, Jørgensen KA, Joergensen KA (1989) Transition-metal-catalyzed epoxidations. Chem Rev 89:431–458. https://doi.org/10.1021/cr00093a001
28. Mitchell JM, Finney NS (2001) New molybdenum catalysts for alkyl olefin epoxidation. Their implications for the mechanism of oxygen atom transfer. J Am Chem Soc 123:862–869. https://doi.org/10.1021/ja002697u
29. Sobczak J, Ziółkowski JJ (1981) The catalytic epoxidation of olefins with organic hydroperoxides. J Mol Catal 13:11–42. https://doi.org/10.1016/0304-5102(81)85028-6
30. Topuzova MG, Kotov SV, Kolev TM (2005) Epoxidation of alkenes in the presence of molybdenum-squarate complexes as novel catalysts. Appl Catal A Gen 281:157–166. https://doi.org/10.1016/j.apcata.2004.11.028
31. Brégeault JM (2003) Transition-metal complexes for liquid-phase catalytic oxidation: some aspects of industrial reactions and of emerging technologies. J Chem Soc Dalt Trans 3:3289–3302. https://doi.org/10.1039/b303073n
32. Punniyamurthy T, Velusamy S, Iqbal J (2005) Recent advances in transition metal catalyzed oxidation of organic substrates with molecular oxygen. Chem Rev 105:2329–2364. https://doi.org/10.1021/cr050523v
33. Ali A, Akram W, Liu HY (2019) Reactive cobalt-oxo complexes of tetrapyrrolic macrocycles and N-based ligand in oxidative transformation reactions. Molecules. https://doi.org/10.3390/molecules24010078
34. Kück JW, Reich RM, Kühn FE (2016) Molecular epoxidation reactions catalyzed by rhenium, molybdenum, and iron complexes. Chem Rec 16:349–364. https://doi.org/10.1002/tcr.201500233
35. Rios LA, Echeverri DA, Franco A (2011) Epoxidation of jatropha oil using heterogeneous catalysts suitable for the prileschajew reaction: acidic resins and immobilized lipase. Appl Catal A Gen 394:132–137. https://doi.org/10.1016/j.apcata.2010.12.033
36. Rios LA, Weckes P, Schuster H, Hoelderich WF (2005) Mesoporous and amorphous Ti-silicas on the epoxidation of vegetable oils. J Catal 232:19–26. https://doi.org/10.1016/j.jcat.2005.02.011
37. Niakan M, Asadi Z, Masteri-Farahani M (2019) Immobilization of salen molybdenum complex on dendrimer functionalized magnetic nanoparticles and its catalytic activity for the epoxidation of olefins. Appl Surf Sci 481:394–403. https://doi.org/10.1016/J.APSUSC.2019.03.088
38. Masteri-Farahani M, Abednatanzi S (2014) Molybdenum complex tethered to the surface of activated carbon as a new recoverable catalyst for the epoxidation of olefins. Appl Catal A Gen 478:211–218. https://doi.org/10.1016/J.APCATA.2014.04.008
39. Environmental Catalysis - 1st Edition - Vicki H. Grassian - Routledge
40. Rodríguez-Padrón D, Puente-Santiago AR, Balu AM et al (2019) Environmental catalysis: present and future. ChemCatChem 11:18–38. https://doi.org/10.1002/cctc.201801248
41. Centi G, Ciambelli P, Perathoner S, Russo P (2002) Environmental catalysis: trends and outlook. Catal Today 75:3–15. 10.1016/S0920-5861(02)00037-8
42. Turco R, Vitiello R, Russo V et al (2013) Selective epoxidation of soybean oil with performic acid catalyzed by acidic ionic exchange resins. Green Process Synth 2:427–434. https://doi.org/10.1515/gps-2013-0045
43. Turco R, Pischetola C, Di Serio M et al (2017) Selective epoxidation of soybean oil in the presence of H-Y zeolite. Ind Eng Chem Res 56:7930–7936. https://doi.org/10.1021/acs.iecr.7b01437
44. Hille R (1996) The mononuclear molybdenum enzymes. Chem Rev 96:2757–2816. https://doi.org/10.1021/cr950061t
45. Hille R (2002) Molybdenum and tungsten in biology. Trends Biochem Sci 27:360–367. https://doi.org/10.1016/S0968-0004(02)02107-2
46. Heinze K (2015) Bioinspired functional analogs of the active site of molybdenum enzymes: intermediates and mechanisms. Coord Chem Rev 300:121–141. https://doi.org/10.1016/j.ccr.2015.04.010
47. Holm RH, Kennepohl P, Solomon EI (1996) Structural and functional aspects of metal sites in biology. Chem Rev 96:2239–2314. https://doi.org/10.1021/cr9500390
48. Martínez H, Cáceres MF, Martínez F et al (2016) Photo-epoxidation of cyclohexene, cyclooctene and 1-octene with molecular oxygen catalyzed by dichloro dioxo-(4,4′-dicarboxylato-2,2′-bipyridine) molybdenum (VI) grafted on mesoporous TiO_2. J Mol Catal A Chem 423:248–255. https://doi.org/10.1016/j.molcata.2016.07.006
49. Arzoumanian H, Castellanos NJ, Martínez FO et al (2010) Silicon-assisted direct covalent grafting on metal oxide surfaces: synthesis and characterization of carboxylate N, N′-ligands on TiO <inf>2</inf>. Eur J Inorg Chem. https://doi.org/10.1002/ejic.200901092
50. Castellanos NJ, Martínez F, Lynen F et al (2013) Dioxygen activation in photooxidation of diphenylmethane by a dioxomolybdenum (VI) complex anchored covalently onto mesoporous titania. Transit Met Chem 38:119–127. https://doi.org/10.1007/s11243-012-9668-2
51. Farias M, Martinelli M, Rolim GK (2011) Immobilized molybdenum acetylacetonate complex on montmorillonite K-10 as catalyst for epoxidation of vegetable oils. Appl Catal A Gen 403:119–127. https://doi.org/10.1016/j.apcata.2011.06.021
52. Bagherzadeh M, Zare M, Salemnoush T et al (2014) Immobilization of dioxomolybdenum (VI) complex bearing salicylidene 2-picoloyl hydrazone on chloropropyl functionalized SBA-15: a highly active, selective and reusable catalyst in olefin epoxidation. Appl Catal A Gen 475:55–62. https://doi.org/10.1016/j.apcata.2014.01.020
53. Castellanos NJ, Martínez F, Páez-Mozo EA et al (2012) Bis (3,5-dimethylpyrazol-1-yl) acetate bound to titania and complexed to molybdenum dioxido as a bidentate N, N′-ligand. Direct comparison with a bipyridyl analog in a photocatalytic arylalkane oxidation by O2. Transit Met Chem 37:629–637. https://doi.org/10.1007/s11243-012-9631-2
54. Zhou HC, Long JR, Yaghi OM (2012) Introduction to metal-organic frameworks. Chem Rev 112:673–674. https://doi.org/10.1021/cr300014x
55. Liu K-G, Sharifzadeh Z, Rouhani F et al (2021) Metal-organic framework composites as green/sustainable catalysts. Coord Chem Rev 436:213827. https://doi.org/10.1016/j.ccr.2021.213827
56. Rowsell JLC, Yaghi OM (2004) Metal-organic frameworks: a new class of porous materials. Microporous Mesoporous Mater 73:3–14. https://doi.org/10.1016/j.micromeso.2004.03.034
57. Ni XL, Liu J, Liu YY et al (2017) Synthesis, characterization and catalytic performance of Mo based metal- organic frameworks in the epoxidation of propylene by cumene hydroperoxide. Chinese Chem Lett 28:1057–1061. https://doi.org/10.1016/j.cclet.2017.01.020
58. Rios Carvajal T (2014) Síntesis y caracterización de redes metal orgánicas (MOF) a partir de ligantes orgánicos tipo fenilen-vinileno modificados con grupos electrodonores. https://repositorio.unal.edu.co/handle/unal/52813

59. Howarth AJ, Liu Y, Li P et al (2016) Chemical, thermal and mechanical stabilities of metal-organic frameworks. Nat Rev Mater 1:1–15. https://doi.org/10.1038/natrevmats.2015.18
60. Liu J, Wu S, Li Z (2018) Recent advances in enzymatic oxidation of alcohols. Curr Opin Chem Biol 43:77–86. https://doi.org/10.1016/j.cbpa.2017.12.001
61. Liu Y-Y, Leus K, Bogaerts T et al (2013) Bimetallic-organic framework as a zero-leaching catalyst in the aerobic oxidation of cyclohexene. ChemCatChem 5:3657–3664. https://doi.org/10.1002/cctc.201300529
62. Kalaj M, Cohen SM (2020) Postsynthetic modification: an enabling technology for the advancement of metal-organic frameworks. ACS Cent Sci 6:1046–1057. https://doi.org/10.1021/acscentsci.0c00690
63. Tanabe KK, Cohen SM (2011) Postsynthetic modification of metal–organic frameworks—a progress report. Chem Soc Rev 40:498–519. https://doi.org/10.1039/c0cs00031k
64. Jiang Y, Liu C, Huang A (2019) EDTA-functionalized covalent organic framework for the removal of heavy-metal ions. ACS Appl Mater Interfaces 11:32186–32191. https://doi.org/10.1021/acsami.9b11850
65. Li GP, Zhang K, Zhang PF et al (2019) Thiol-functionalized pores via post-synthesis modification in a metal-organic framework with selective removal of Hg(II) in water. Inorg Chem 58:3409–3415. https://doi.org/10.1021/acs.inorgchem.8b03505
66. Castellanos NJ, Martinez Rojas Z, Camargo HA et al (2019) Congo red decomposition by photocatalytic formation of hydroxyl radicals (–OH) using titanium metal–organic frameworks. Transit Met Chem 44:77–87. https://doi.org/10.1007/s11243-018-0271-z
67. Nagatomi H, Gallington LC, Goswami S et al (2020) Regioselective functionalization of the mesoporous metal−organic framework, NU-1000, with photo-active tris-(2,2′bipyridine) ruthenium(II). ACS Omega 5:30299–30305. https://doi.org/10.1021/acsomega.0c04823
68. Bobb JA, Ibrahim AA, El-Shall MS (2018) Laser synthesis of carbonaceous TiO_2 from metal-organic frameworks: optimum support for Pd nanoparticles for C–C cross-coupling reactions. ACS Appl Nano Mater 1:4852–4862. https://doi.org/10.1021/acsanm.8b01045
69. Xi FG, Liu H, Yang NN, Gao EQ (2016) Aldehyde-tagged zirconium metal-organic frameworks: a versatile platform for postsynthetic modification. Inorg Chem 55:4701–4703. https://doi.org/10.1021/acs.inorgchem.6b00598
70. Zhang L, Yuan S, Fan W et al (2019) Cooperative sieving and functionalization of Zr metal-organic frameworks through insertion and post-modification of auxiliary linkers. ACS Appl Mater Interfaces 11:22390–22397. https://doi.org/10.1021/acsami.9b05091
71. Wang T, Song X, Xu H et al (2021) Recyclable and magnetically functionalized metal-organic framework catalyst: IL/Fe 3 O 4 @ HKUST-1 for the cycloaddition reaction of CO_2 with epoxides. ACS Appl Mater Interfaces 13:22836–22844. https://doi.org/10.1021/acsami.1c03345
72. Ji H, Naveen K, Lee W et al (2020) Pyridinium-functionalized ionic metal-organic frameworks designed as bifunctional catalysts for CO_2 fixation into cyclic carbonates. ACS Appl Mater Interfaces 12:24868–24876. https://doi.org/10.1021/acsami.0c05912
73. Tang Q, Li Q, Pan X et al (2021) Poly(acrylated epoxidized soybean oil)-modified carbon nanotubes and their application in epoxidized soybean oil-based thermoset composites. Polym Compos 42:5774–5788. https://doi.org/10.1002/PC.26259
74. Wu Y, Li K (2018) Acrylated epoxidized soybean oil as a styrene replacement in a dicyclopentadiene-modified unsaturated polyester resin. J Appl Polym Sci. https://doi.org/10.1002/APP.46212
75. Turco R, Pischetola C, Tesser R et al (2016) New findings on soybean and methylester epoxidation with alumina as the catalyst. RSC Adv 6:31647–31652. https://doi.org/10.1039/c6ra01780k
76. Olivieri GV, De Quadros JV, Giudici R (2020) Epoxidation reaction of soybean oil: experimental study and comprehensive kinetic modeling. Ind Eng Chem Res 59:18808–18823. https://doi.org/10.1021/acs.iecr.0c03847
77. Leus K, Liu YY, Meledina M et al (2014) A MoVI grafted metal organic framework: synthesis, characterization and catalytic investigations. J Catal 316:201–209. https://doi.org/10.1016/j.jcat.2014.05.019
78. Liu YY, Decadt R, Bogaerts T et al (2013) Bipyridine-based nanosized metal-organic framework with tunable luminescence by a postmodification with Eu (III): an experimental and theoretical study. J Phys Chem C 117:11302–11310. https://doi.org/10.1021/jp402154q
79. Tubino M, Aricetti JA (2013) A green potentiometric method for the determination of the iodine number of biodiesel. Fuel 103:1158–1163. https://doi.org/10.1016/j.fuel.2012.10.011
80. Of A, Fats C (1997) Oxirane Oxygen. AOCS Off Method CD 9-57 8–9
81. Miyake Y, Yokomizo K, Matsuzaki N (1998) Determination of unsaturated fatty acid composition by high-resolution nuclear magnetic resonance spectroscopy. J Am Oil Chem Soc 75:1091–1094. https://doi.org/10.1007/s11746-998-0295-1
82. Aerts HAJ, Jacobs PA (2004) Epoxide yield determination of oils and fatty acid methyl esters using 1H NMR. JAOCS, J Am Oil Chem Soc 81:841–846. https://doi.org/10.1007/s11746-004-0989-1
83. Liu YY, Leus K, Sun Z et al (2019) Catalytic oxidative desulfurization of model and real diesel over a molybdenum anchored metal-organic framework. Microporous Mesoporous Mater 277:245–252. https://doi.org/10.1016/j.micromeso.2018.11.004
84. D'Amico ML, Rasmussen K, Sisneros D et al (1992) Epoxidation of cyclic olefins using dimeric molybdenum (VI) catalysts. Inorganica Chim Acta 191:167–170. https://doi.org/10.1016/S0020-1693(00)93456-X
85. Arzoumanian H (2012) Molybdenum-oxo and peroxo complexes in oxygen atom transfer processes with O_2 as the primary oxidant. Curr Inorg Chem 1:140–145. https://doi.org/10.2174/1877944111101020140
86. Arzoumanian H (1998) Molybdenum-oxo chemistry in various aspects of oxygen atom transfer processes. Coord Chem Rev 178–180:191–202. https://doi.org/10.1016/s0010-8545(98)00056-3
87. Farias M, Martinelli M, Bottega DP (2010) Epoxidation of soybean oil using a homogeneous catalytic system based on a molybdenum (VI) complex. Appl Catal A Gen 384:213–219. https://doi.org/10.1016/j.apcata.2010.06.038
88. Rezaeifard A, Sheikhshoaie I, Monadi M, Stoeckli-Evans H (2010) Synthesis, crystal structure, and catalytic properties of novel dioxidomolybdenum (VI) complexes with tridentate schiff base ligands in the biomimetic and highly selective oxygenation of alkenes and sulfides. Eur J Inorg Chem. https://doi.org/10.1002/ejic.200900814
89. Kühn FE, Groarke M, Bencze É et al (2002) Octahedral bipyridine and bipyrimidine dioxomolybdenum (VI) complexes: characterization, application in catalytic epoxidation, and density functional mechanistic study. Chem—A Eur J 8:2370–2383. https://doi.org/10.1002/1521-3765(20020517)8:10%3c2370::AID-CHEM2370%3e3.0.CO;2-A
90. Sobczak JM, Ziółkowski JJ (2003) Molybdenum complex-catalysed epoxidation of unsaturated fatty acids by organic hydroperoxides. Appl Catal A Gen 248:261–268. https://doi.org/10.1016/S0926-860X(03)00165-0
91. Salavati-Niasari M, Bazarganipour M (2007) Effect of single-wall carbon nanotubes on direct epoxidation of cyclohexene

catalyzed by new derivatives of cis-dioxomolybdenum(VI) complexes with bis-bidentate Schiff-base containing aromatic nitrogen-nitrogen linkers. J Mol Catal A Chem 278:173–180. https://doi.org/10.1016/j.molcata.2007.09.009
92. Wang G, Chen G, Luck RL et al (2004) New molybdenum(VI) catalysts for the epoxidation of cyclohexene: synthesis, reactivity and crystal structures. Inorganica Chim Acta 357:3223–3229. https://doi.org/10.1016/J.ICA.2004.03.030
93. Mu B, Walton KS (2011) Thermal analysis and heat capacity study of metal-organic frameworks. J Phys Chem C 115:22748–22754. https://doi.org/10.1021/jp205538a
94. Pineda Beltran RA (2018) Uso de la oxidación catalítica del acetaldehído en la epoxidación de aceites vegetales. https://repositorio.unal.edu.co/handle/unal/76204
95. Lindley MG (1998) The impact of food processing on antioxidants in vegetable oils, fruits and vegetables. Food Sci Technol 9:336–340. 10.1016/S0924-2244(98)00050-8
96. Miao YX, Liu JP (2014) Epoxidation of soybean oil under acid-free condition. Adv Mater Res 881–883:140–143. https://doi.org/10.4028/www.scientific.net/AMR.881-883.140
97. Jiang J, Zhang Y, Yan L, Jiang P (2012) Epoxidation of soybean oil catalyzed by peroxo phosphotungstic acid supported on modified halloysite nanotubes. Appl Surf Sci 258:6637–6642. https://doi.org/10.1016/j.apsusc.2012.03.095
98. Wai PT, Jiang P, Shen Y et al (2020) Entrapment of peroxophosphotungstate in SBA-15 by silylation and its catalytic efficiency in the epoxidation of soybean oil. Appl Catal A Gen 596:117537. https://doi.org/10.1016/J.APCATA.2020.117537
99. Cai L, Chen C, Wang W et al (2020) Acid-free epoxidation of soybean oil with hydrogen peroxide to epoxidized soybean oil over titanium silicalite-1 zeolite supported cadmium catalysts. J Ind Eng Chem 91:191–200. https://doi.org/10.1016/J.JIEC.2020.07.052
100. Lage FC, Suzuki AH, Oliveira LS (2021) Comparative evaluation of conventional and microwave assisted epoxidation of soybean oil with citric acid, acetic acid using homogeneous and heterogeneous catalysis. Brazilian J Chem Eng 38:327–340. https://doi.org/10.1007/s43153-021-00096-4
101. Zhang M, Cheng Q, Chen T et al (2022) Development and characterisation research on SnO2-Al2 O3-NiO/SO4 2À catalysed epoxidation of soybean oil under hydraulic cavitation epoxidation, hydraulic cavitation SnO 2-Al2 O3-NiO/SO4 2À. Appl Organomet Chem. https://doi.org/10.1002/aoc.6617
102. Martinez QH, Amaya ÁA, Paez-Mozo EA et al (2020) Photo-assisted O-atom transfer to monoterpenes with molecular oxygen and a dioxoMo(VI) complex immobilized on TiO_2 nanotubes. Catal Today. https://doi.org/10.1016/j.cattod.2020.07.053
103. Martínez H, Amaya ÁA, Páez-Mozo EA, Martínez OF (2018) Highly efficient epoxidation of alfa-pinene with O_2 photocatalyzed by dioxo Mo(VI) complex anchored on TiO_2 nanotubes. Microporous Mesoporous Mater 265:202–210. https://doi.org/10.1016/j.micromeso.2018.02.005
104. Martínez QH, Paez-Mozo EA, Martínez OF (2021) Selective Photo-epoxidation of (R)-(+)- and (S)-(−)-Limonene by Chiral and Non-Chiral Dioxo-Mo(VI) Complexes Anchored on TiO2-Nanotubes. Top Catal 64:36–50. https://doi.org/10.1007/s11244-020-01355-3
105. Wai PT, Jiang P, Shen Y et al (2019) Catalytic developments in the epoxidation of vegetable oils and the analysis methods of epoxidized products. RSC Adv 9:38119–38136. https://doi.org/10.1039/C9RA05943A
106. Grünert W, Stakheev AY, Feldhaus R et al (1991) Analysis of Mo(3d) XPS spectra of supported Mo catalysts: An alternative approach. J Phys Chem 95:1323–1328. https://doi.org/10.1021/j100156a054